Anal Bioanal Chem (2013) 405:1303–1310
DOI 10.1007/s00216-012-6541-2

ORIGINAL PAPER

Identification of PET radiometabolites by cytochrome P450, UHPLC/Q-ToF-MS and fast radio-LC: applied to the PET radioligands [^{11}C]flumazenil, [^{18}F]FE-PE2I, and [^{11}C]PBR28

Nahid Amini · Ryuji Nakao · Magnus Schou · Christer Halldin

Received: 3 October 2012 / Accepted: 31 October 2012 / Published online: 21 November 2012

Abstract A general method is presented for the identification of radiometabolites in plasma of human and monkey subjects after administration of positron emission tomography (PET) radioligands. The radiometabolites are first produced in vitro, using liver microsomes, subsequently separated using fast radio-liquid chromatography (radio-LC), and individually collected and identified by ultra high-performance liquid chromatography/quadrupole-time of flight-mass spectrometry in MS and MS^E mode. Fast radio-LC provided superior resolution compared to conventional radio-LC, resulting in separation of a greater number of metabolites. The radiometabolites produced in vivo are then compared to and identified based on the in vitro results. This approach was applied to three PET radioligands, [^{11}C] flumazenil, [^{18}F]FE-PE2I, and [^{11}C]PBR28, resulting in the identification of five, two, and one radiometabolites, respectively. This procedure can easily be adopted to identify the radiometabolites produced in vivo from a variety of PET radioligands.

Keywords Positron emission tomography (PET) radioligands · Radiometabolites · Fast radio-liquid chromatography (radio-LC) · Ultra high-performance liquid chromatography/quadrupole-time of flight-mass spectrometry (UHPLC/Q-ToF-MS) · Cytochrome P450

N. Amini (✉) · R. Nakao · M. Schou · C. Halldin
Department of Clinical Neuroscience, Center for Psychiatric Research, Karolinska Institutet, Stockholm 171 76, Sweden
e-mail: nahid.amini@ki.se

M. Schou
AstraZeneca, Research & Development, Innovative Medicines, CNSP iMed, 151 85 Södertälje, Sweden

Introduction

Positron emission tomography (PET) is a sensitive in vivo imaging technique in which compounds with short-lived radionuclides such as ^{11}C ($t_{1/2}$=20.4 min) and ^{18}F ($t_{1/2}$= 109.8 min) are administered and used for quantitative measurements of biochemical processes. However, a drawback with PET is that it only reflects the total amount of radioactivity in tissue and does not provide any information on its chemical form. The presence of radiometabolites in the tissue to be imaged would influence the accurate quantification of a PET measurement [1, 2]. Therefore, it is important to develop methods by which radiometabolites of radioligands, especially those with the potential of crossing the blood brain barrier, can be identified and measured over time. Identification of radiometabolites during development of new radioligands is also of significance since it would provide information as to the most appropriate position to radiolabel a compound to avoid formation of interfering radiometabolites [3, 4].

Since PET radioligands are mainly metabolized in the liver during a PET scan, hepatic microsomes are suitable for studying their metabolism in vitro [5]. To elucidate the structure of these radiometabolites, liquid chromatography/mass spectrometry (LC/MS) is commonly applied providing mass/charge (m/z) values for radioligands and their produced fragments [6, 7]. Using a time of flight (ToF), mass spectrometer has the further advantage of providing accurate m/z values and therefore more precise identification of unknown compounds. This information can then be employed to identify the relative composition of radiometabolites in vivo.

In PET studies, liquid chromatography coupled to radioactivity detector (radio-LC) is often used to separate and measure the concentration of radioligands and their radiometabolites. Semi-preparative LC columns are commonly

employed for this purpose; however, they may not provide the resolution required to separate the radiometabolites from one another, and due to their relatively long analysis time problems associate with low radioactivity can occur, especially at the late time points of PET imaging studies. An alternative method is fast radio-LC, in which shorter columns with smaller particle size are employed, resulting in increased sensitivity, separation efficiency, and shorter analysis time [8].

The objective of this work was to establish a method by which radiometabolites of radioligands formed in vivo can be identified and measured with the aid of hepatic microsomes, fast radio-LC, and ultra high-performance liquid chromatography/quadrupole-time of flight-mass spectrometry (UHPLC/Q-ToF-MS). One commonly used radioligand, [^{11}C]flumazenil, and two newly developed ones, [^{18}F]FE-PE2I and [^{11}C]PBR28, Fig. 1, were chosen to demonstrate the applicability of the developed method. [^{11}C]Flumazenil [9–11] is used for imaging of central benzodiazepine receptors in brain, while [^{18}F]FE-PE2I [12] and [^{11}C]PBR28 [13] are dopamine transporter and brain 18 kDa translocator protein (TSPO) PET radioligands, respectively.

Experimental

Materials

The precursors and standards of flumazenil, FE-PE2I, and PBR28 were purchased from PharmaSynth AS (Estonia). Acetonitrile and water (both LC/MS grade) were from Fisher Scientific and 2-methoxybenzoic acid, phosphoric acid, and ammonium formate were from Sigma-Aldrich. Formic acid and leucine enkephalin were purchased from Sigma and Merck, respectively.

Pooled monkey liver microsomes (MLM) and Ultrapool™ human liver microsomes (HLM) from 150 mixed gender donors were purchased from BD Biosciences. NADPH regenerating system consisting of two solutions, $NADP^+$ plus glucose-6-phosphate and glucose 6-phosphate dehydrogenase, as well as 0.5 M sodium phosphate buffer pH7.4 were also from BD Biosciences.

Microsome incubation procedure

The incubations were conducted at 37 °C with 0.5 mg/mL of microsomal protein, either MLM or HLM, in the presence of 1.5 mM $NADP^+$, 3.3 mM glucose-6-phosphate, 3.3 mM $MgCl_2$, and 0.4 U/mL glucose 6-phosphate dehydrogenase in 100 mM phosphate buffer pH7.4. In carrier-added experiments, 2 μL of a 5-mM solution of the ligand of interest as well as 10 μL of the radio-labeled ligand were added to incubation mixture. The final volume of incubation solution was 1 mL making the concentration of the carrier in the carrier-added solutions equal to 10 μM. To terminate the reaction at a certain time point, 200 μL of the incubation mixture was added to the same volume of cold acetonitrile. The protein was removed by centrifugation at 10,000×*g* for 4 min at 4 °C, and approximately 1 mL of water was added to the supernatant before injection into the fast radio-LC system.

Fast and conventional radio-LC systems

Both carrier-added and no carrier-added radioligand incubation mixtures, as well as plasma samples from monkey and human subjects were analyzed by fast radio-LC. Chromatographic separation was performed on an XBridge C_{18} column (Waters, 50×10 mm inner diameter (I.D.), 2.5 μm+guard 10×10 mm I.D., 5 μm) at a flow rate of 6 mL/min using an Agilent binary pump coupled to a fraction collector (Agilent 1200 series) and a radiation detector (Oyokoken, S-2493Z). The mobile phase consisted of (A) 0.1 % formic acid in water and (B) 0.1 % formic acid in acetonitrile. In the case of [^{11}C]flumazenil and [^{18}F]FE-PE2I, the elution profile used started from 15 % B and continued isocratic for 4 min and then reached 40 % B after 6 min. [^{11}C]PBR28 was eluted with a gradient starting from 15 % B and reaching 40 % B after 6 min and remaining on 40 % B for extra 2 min. The peaks corresponding to the parent radioligands and their radiometabolites were collected by the fraction collector.

Fig. 1 The investigated PET radioligands

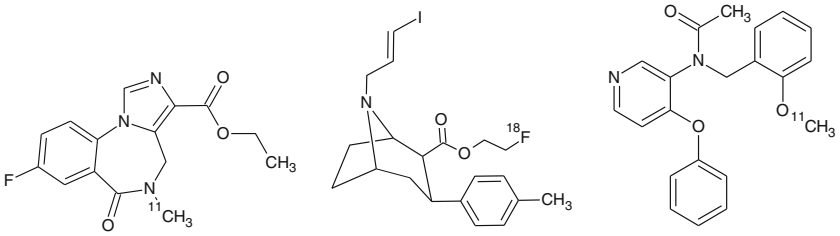

[^{11}C]flumazenil [^{18}F]FE-PE2I [^{11}C]PBR28

The monkey and human PET studies were approved by the Regional Ethics Committee and by the Animal Research Ethical Committee in Stockholm. Blood samples were taken at pre-specified time points and centrifuged at 2,000×*g* for 2–4 min at room temperature to separate plasma (0.2–0.5 mL). The protein in the plasma samples was denaturated by addition of 1.4 times volume of acetonitrile. After stirring with a vortex mixer, the samples were centrifuged at 2,000×*g* for 4 min at room temperature and approximately 4 mL of water was added to the supernatant plasma-acetonitrile mixture, which was then injected into both the fast and conventional radio-LC systems. A semi-preparative LC column (μBondapak C18, Waters, 300×7.8 mm I.D., 10 μm) was used in the conventional radio-LC setup. The mobile phase consisted of acetonitrile (C) and 10 mM phosphoric acid (D) in the analysis of [^{11}C]flumazenil and [^{18}F] FE-PE2I according to the following gradients, respectively, 15 % C to 60 % C in 5 min, 60 % C at 8 min and 25 % C to 80 % C in 4.5 min, and 30 % C at 8 min. [^{11}C]PBR28 and its radiometabolites were separated using a gradient starting from 40 % acetonitrile and 60 % ammonium formate (10 mM), reaching 80 % acetonitrile after 4 min and staying isocratic for another 4 min. The flow rate used in the conventional radio-LC system was 6 mL/min.

LC/MS method

The analyses were performed on a Waters (Milford, MA, USA) Acquity Ultra Performance LC™ binary solvent manager coupled to a PDA detector and Waters (Micromass UK Limited, Manchester, UK) Q-Tof Premeir™. All the samples (10 μL) were injected onto a Waters 50×2.1 mm I.D., 1.7 μm Ethylene Bridged Hybrid (BEH) C_{18} column and eluted using a 10-min linear gradient starting from 100 % water containing 0.1 % formic acid and ending by 35 % acetonitrile containing 0.1 % formic acid at a flow rate of 0.5 mL/min. Positive electrospray ionization in V-mode with extended dynamic range was used. Two scan functions, MS and MS^E, in the mass range of 50–1,000 Da were performed simultaneously under the following conditions for FE-PE2I samples: capillary 4.5 kV, sampling cone 45 V, extraction cone 4.5 V, source temperature 100 °C, and desolvation temperature 380 °C. For samples containing flumazenil and PBR28, the capillary and sampling cone were set to 3.5 kV and 25 V, respectively. The collision energy was set to 5 V during the MS acquisition and it was ramped from 10 to 45 V during the MS^E acquisition. MS/MS was only performed for two of FE-PE2I metabolites having identical retention times, *m*/*z* 322.1459 and *m*/*z* 308.1652. Leucine enkephalin was used as the lock mass (*m*/*z* 556.2771) at a concentration of 500 pg/μL and a flow rate of 30 μL/min. MetaboLynx (Waters, Milford, MA, USA) was used to aid in metabolite identification.

Radioligand synthesis

[^{11}C]Flumazenil and [^{11}C]PBR28 were synthesized by methylation of their desmethyl precursors using [^{11}C]methyl triflate [14] and [^{11}C]methyl iodide [15], respectively. [^{18}F] FE-PE2I was produced by direct ^{18}F-fluorination of the tosyl precursor as described in details elsewhere [16].

Results and discussion

Separation and collection of in vitro radiometabolites by fast radio-LC

To identify phase I radiometabolites of the PET radioligands investigated here, carrier-added solutions of [^{11}C]flumazenil, [^{18}F]FE-PE2I, and [^{11}C]PBR28 were each incubated with either monkey or human liver microsomes depending on the availability of the plasma samples used further on for in vivo studies. When producing metabolites in vitro, it is important to use microsomes originating from the same species as the in vivo study will be performed on, given that metabolic profiles are species dependent [17]. The addition of carrier was essential for performing LC/MS analysis in the next stage due to the very low concentration of the radioligands (typically in the range of 2–100 fmol/mL plasma) and their subsequent radiometabolites. Metabolism was stopped at various time points and samples were analyzed by fast radio-LC. The produced radiometabolites as well as the radioligands were collected and identified by UHPLC/Q-ToF-MS as described below.

Radiometabolite identification by UHPLC/Q-ToF-MS

The monoisotopic masses of each radioligand, its radiometabolites, and their fragments were determined by acquiring total ion chromatograms in MS and MS^E mode simultaneously. The use of MS^E saved analysis time and sample while providing nearly the same information as MS/MS [18]. The mass errors obtained for the parent and fragment ions were less than 5 and 10 ppm, respectively.

The fragmentation pattern observed here for flumazenil is similar to what has been obtained by atmospheric pressure chemical ionization [19] producing an acylium ion (*m*/*z* 258.0691). The two radiometabolites identified for flumazenil, a hydroxyl-ethyl ester (flumazenil-M1) and an acidic (flumazenil-M2), revealed identical fragments to flumazenil. The occurrence of these radiometabolites in plasma of primates and humans has been reported [11, 20–22].

Table 1 List of PET radioligands used in this study and their radiometabolites identified by UHPLC/Q-ToF-MS, including retention times, measured masses of parent and fragment ions, and proposed losses from parents

Chemical structure	Abbreviation	R_t (min)	Precursor ion measured *(m/z)*	Most abundant fragment ions measured *(m/z)*	Proposed loss from parent
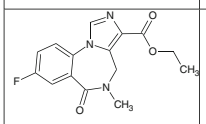	Flumazenil	5.8	304.1081	258.0691 229.0643 217.0660 189.0709	C_2H_6O $C_3H_7O_2$ $C_4H_7O_2$ $C_5H_7O_3$
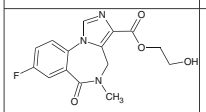	Flumazenil-M1	4.2	320.1050	258.0690 229.0644 217.0660 189.0710	$C_2H_6O_2$ $C_3H_7O_3$ $C_4H_7O_3$ $C_5H_7O_4$
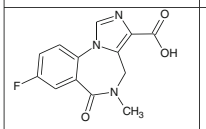	Flumazenil-M2	3.2	276.0767	258.0691 229.0642 217.0658 189.0711	H_2O CH_3O_2 $C_2H_3O_2$ $C_3H_3O_3$
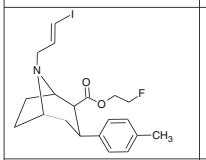	FE-PE2I	7.8	458.0996	394.0652 366.0728 247.9946 166.9350	C_2H_5OF $C_3H_5O_2F$ $C_{12}H_{15}O_2F$ $C_{17}H_{22}NO_2F$
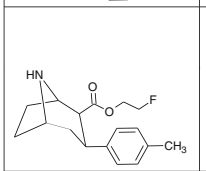	FE-PE2I-M1	5.9	292.1720	228.1378 169.1111 147.0803 105.0691 82.0649 70.0663	C_2H_5OF C_8H_8F $C_7H_{12}NOF$ $C_9H_{14}NO_2F$ $C_{12}H_{15}O_2F$ $C_{13}H_{15}O_2F$
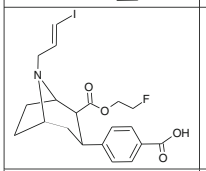	FE-PE2I-M2	4.7	488.0737	424.0452 396.0468 360.1581 166.9357	C_2H_5OF $C_3H_5O_2F$ HI $C_{17}H_{20}NO_4F$
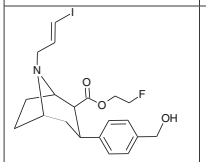	FE-PE2I-M3	4.6	474.0939	456.0878 410.0635 382.0665 247.9952 166.9373	H_2O C_2H_5OF $C_3H_5O_2F$ $C_{11}H_{15}O_2F$ $C_{17}H_{22}NO_3F$
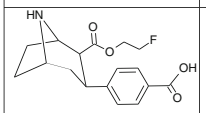	FE-PE2I-M4	2.5	322.1459	258.1121 230.0822 135.0442 82.0652 70.0655	C_2H_5OF C_4H_9OF $C_9H_{14}NO_2F$ $C_{12}H_{13}O_4F$ $C_{13}H_{13}O_4F$
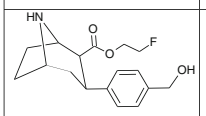	FE-PE2I-M5	2.5	308.1652	244.1328 226.1238 155.0932 121.0642 82.0660 70.0651	C_2H_5OF $C_2H_7O_2F$ $C_9H_{10}OF$ $C_9H_{14}NO_2F$ $C_{12}H_{15}O_3F$ $C_{13}H_{15}O_3F$
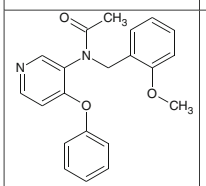	PBR28	8.4	349.1541	188.0714 121.0641 93.0696 91.0541	$C_{10}H_{11}NO$ $C_{13}H_{12}N_2O_2$ $C_{14}H_{12}N_2O_3$ $C_{14}H_{14}N_2O_3$
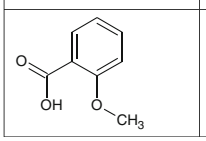	PBR28-M1	3.7	153.0539	135.0446 92.0258	H_2O $C_2H_5O_2$

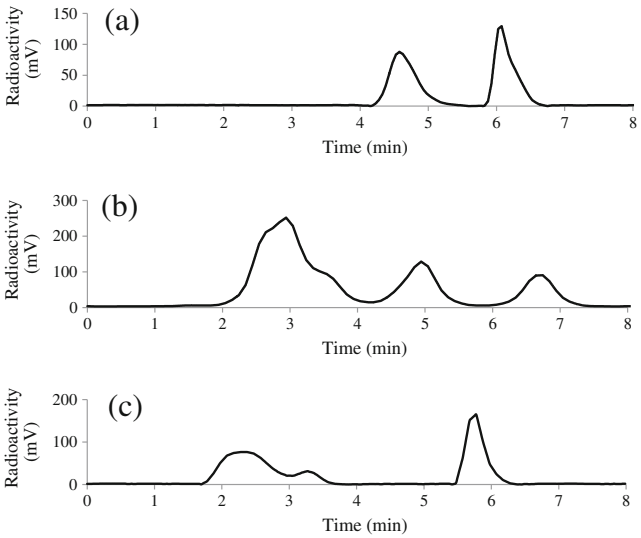

Fig. 2 Conventional radio-LC chromatograms of (**a**) rhesus monkey plasma collected 20 min after administration of [^{11}C]flumazenil, (**b**) rhesus monkey plasma collected 20 min after administration of [^{18}F]FE-PE2I, and (**c**) human plasma collected 10 min after administration of [^{11}C]PBR28

In the case of FE-PE2I, the five major radiometabolites observed were as a result of *N*-dealkylation, benzylic hydroxylation, and further oxidation of the benzyl alcohol by CYP450 enzymes. Similar metabolism has been reported for a structurally related compound, PE2I [6]. LC/MS generated molecular ions *m/z* 292.1720, loss of C_3H_3I; *m/z* 488.0737, methyl oxidation to carboxylic acid; and *m/z* 474.0939, benzyl hydroxylation as listed in Table 1. The proposed structures for the radiometabolites were further confirmed by their generated fragments. FE-PE2I generated fragments *m/z* 394.0652 and *m/z* 366.0728 corresponding to the loss of C_2H_5OF and $C_3H_5O_2F$, respectively. FE-PE2I-M2 produced fragments *m/z* 424.0452 and *m/z* 396.0468, approximately 30 mass units higher than the fragments produced by FE-PE2I, indicating the preservation of carboxylic acid in each fragment. The fragments *m/z* 410.0635 and *m/z* 382.0665 produced from FE-PE2I-M3 show an increase of approximately 16 mass units compared to the fragments from FE-PE2I. The presence of the hydroxyl group on benzyl, and not on benzene [23], is confirmed by the formation of fragment *m/z* 456.0878 owing to loss of H_2O from FE-PE2I-M3.

PBR28-M1 was generated from N-debenzylation of PBR28 followed by oxidation of the [^{11}C]2-methoxybenzaldehyde. The presence of this radiometabolite was further confirmed by comparing its retention time and fragmentation to a standard reference solution. PBR28-M1 has been previously detected in vivo in rats [13].

In vivo identification of radiometabolites

Plasma samples from rhesus monkey, after administration of [^{11}C]flumazenil and [^{18}F]FE-PE2I, and from human after administration of [^{11}C]PBR28 were collected at different time points and analyzed using both conventional radio-LC (Fig. 2)

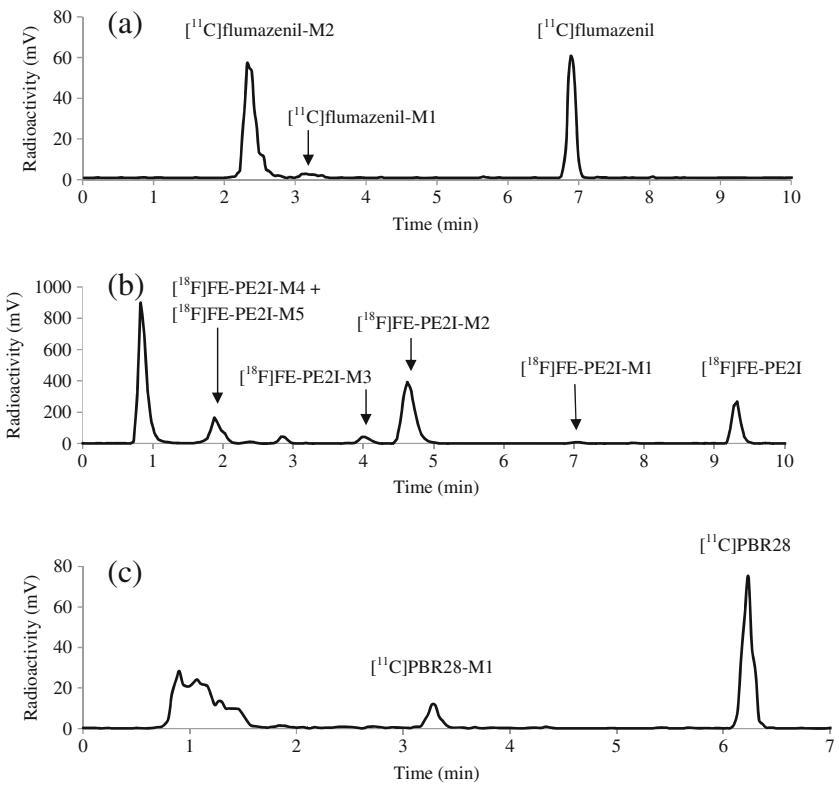

Fig. 3 Fast radio-LC chromatograms of (**a**) rhesus monkey plasma collected 20 min after administration of [^{11}C]flumazenil, (**b**) rhesus monkey plasma collected 20 min after administration of [^{18}F]FE-PE2I, and (**c**) human plasma collected 10 min after administration of [^{11}C]PBR28. The radioligands and their identified radiometabolites are marked on each chromatogram

and fast radio-LC (Fig. 3). The fast radio-LC was superior to the conventional radio-LC system in separating radiometabolites of the PET radioligands. The two radiometabolites separated and identified by fast radio-LC after administration of [^{11}C]flumazenil (Fig. 3(a)) appeared as a single radiometabolite when using conventional radio-LC (Fig. 2(a)). Nevertheless, this might have been due to the low abundance of [^{11}C]flumazenil-M1. In Fig. 2(b), only two peaks corresponding to radiometabolites of [^{18}F]FE-PE2I were observed, as previously reported [24, 25]. However, by using fast radio-LC, seven radiometabolites were separated, of which five were identified (Fig. 3(b)). The radiometabolite of [^{11}C]PBR28 with closest lipophilicity to the parent (Fig. 3(c)) was also separated and identified using fast radio-LC. This radiometabolite coeluted with the more polar radiometabolites when conventional radio-LC was employed and the sum has been previously measured and reported as a single radiometabolite [26, 27]. In all cases, identification was based on comparing retention times to the corresponding CYP450 incubation of radioligand as well as co-injection of plasma samples with solutions containing radiometabolites of interest produced by CYP450 enzymes. In most cases, lipophilic radiometabolites are often of higher interest due to their potential of passing the blood–brain barrier and interfering with the quantitative analysis of the target receptors [28].

Metabolic stability

The metabolic stability of the three radioligands of interest in vitro (no carrier-added) and in vivo is demonstrated in Figs. 4

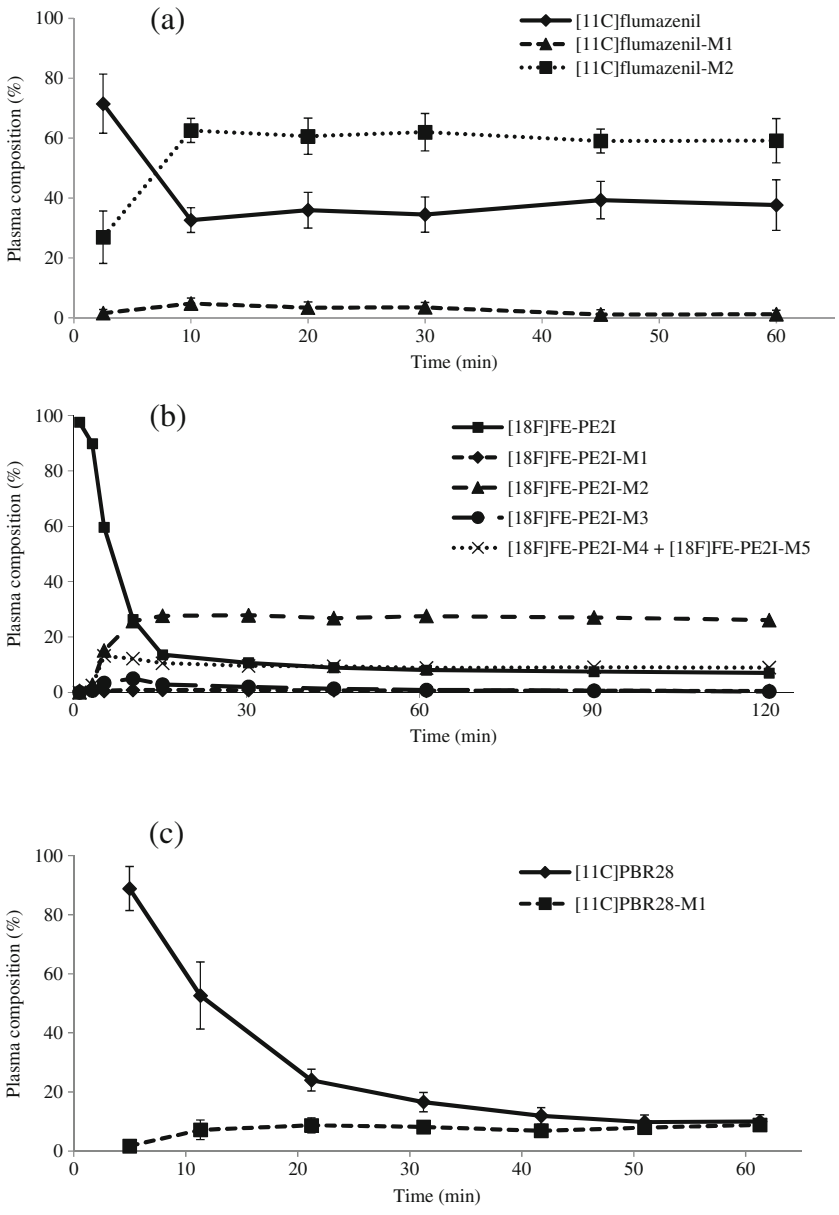

Fig. 4 Time course of radioactivity composition of investigated radioligands and their identified radiometabolites after administration of (**a**) [^{11}C] flumazenil into four rhesus monkeys, (**b**) [^{18}F]FE-PE2I into a rhesus monkey, and (**c**) [^{11}C] PBR28 into three humans

and 5. The quantity of unchanged parent radioligand and produced radiometabolites are stated as a percentage of the sum of areas of all the detected radioactive peaks. In the case of [^{11}C] flumazenil (Figs. 4(a) and 5(a)), the radioligand is metabolized faster in vivo than in vitro. However, the opposite is observed for [^{18}F]FE-PE2I (Figs. 4(b) and 5(b)), and [^{11}C]PBR28 (Figs. 4 (c) and 5(c)). With [^{11}C]flumazenil, [^{11}C]flumazenil-M2 is the major radiometabolite produced both in vivo and in vitro. In vivo, [^{18}F]FE-PE2I-M2 is the major radiometabolite produced in contrary to the in vitro results where the combination of [^{18}F] FE-PE2I-M4 and [^{18}F]FE-PE2I-M5 is dominant. Discrepancies in the metabolites produced in vivo and in vitro are reported elsewhere too [29, 30]. The number of radiometabolites produced by microsome incubation of [^{11}C]flumazenil and [^{18}F]

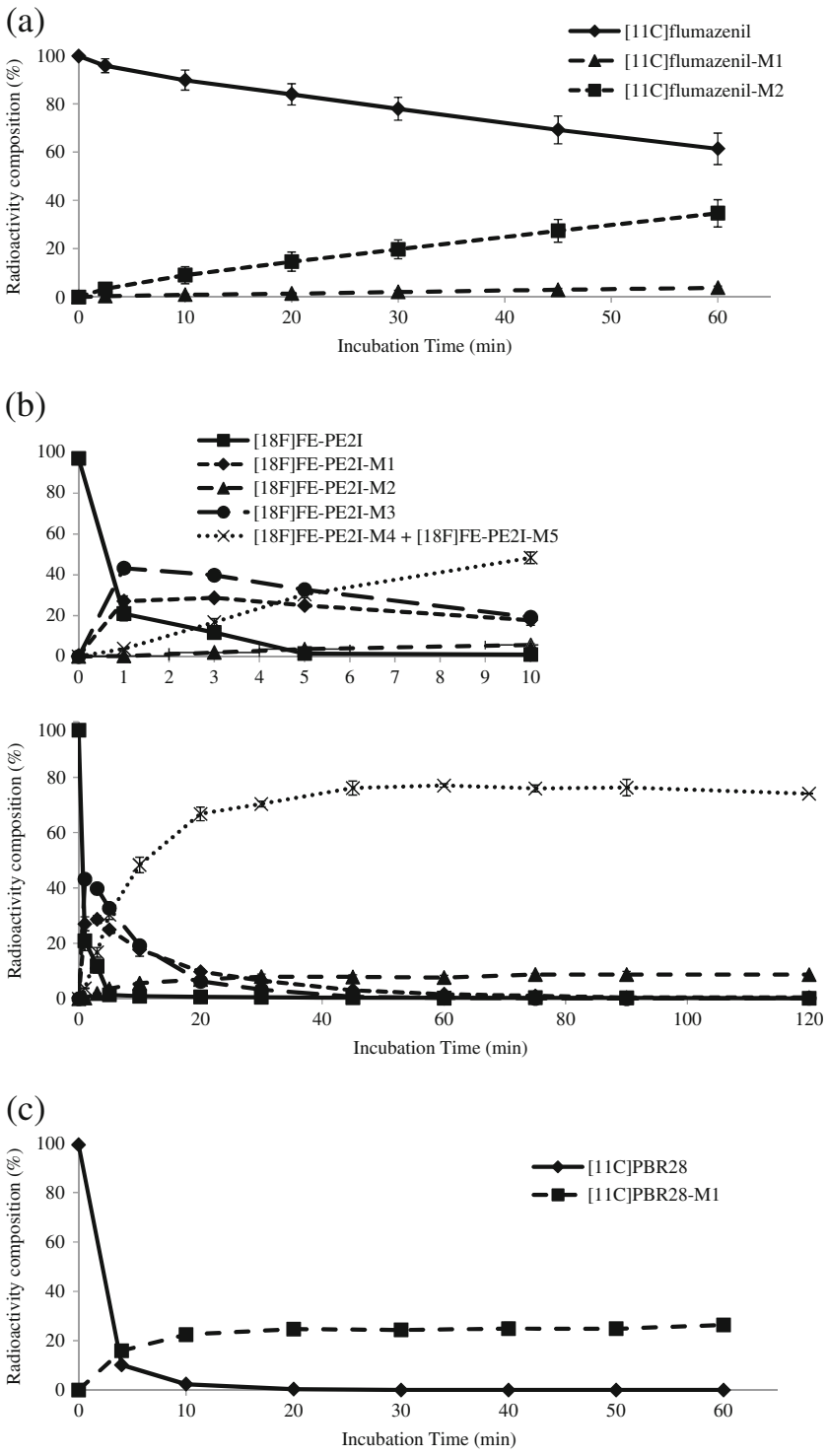

Fig. 5 Mean time course of radioactivity composition of investigated radioligands and their identified radiometabolites in vitro, n=3. (**a**) Incubation of [^{11}C]flumazenil with monkey liver microsomes, (**b**) incubation of [^{18}F]FE-PE2I with monkey liver microsomes, and (**c**) incubation of [^{11}C] PBR28 with human liver microsomes

FE-PE2I was equal to what was observed in plasma, yet incubation of [^{11}C]PBR28 resulted in four extra radiometabolites which were not observed in human plasma. In microsome incubation studies, no radioactive metabolites were observed in the absence of microsomes, illustrating that all the observed radiometabolites resulted from microsome-dependent reactions.

In vitro metabolism, using liver microsomes of different species, was successfully employed to predict and identify the in vivo radiometabolites. However in general, it was not possible to predict the relative amount of radiometabolites produced in vivo using the in vitro method.

Conclusions

A method by which radiometabolites of PET radioligands produced in vivo are identified and measured over time was developed. The superior separation of radiometabolites, compared to conventional methods, was achieved by fast radio-LC while the UHPLC/Q-ToF-MS provided exact mass-to-charge ratios of the radiometabolites and their fragments leading to their identification.

Acknowledgments The authors thank all the members of the PET group at Karolinska Institutet for their kind assistance during this study.

References

1. Halldin C, Swahn C-G, Farde L, Sedvall G (1995) In: Comar D (ed) PET for drug development and evaluation. Kluwer Academic, Netherlands
2. Price JC, Lopresti BJ, Meltzer CC, Smith GS, Mason NS, Huang Y, Holt DP, Gunn RN, Mathis CA (2001) Synapse 41:11–21
3. Osman S, Lundkvist C, Pike VW, Halldin C, McCarron JA, Swahn CG, Ginovart N, Luthra SK, Bench CJ, Grasby PM, Wikström H, Barf T, Cliffe IA, Fletcher A, Farde L (1996) Nucl Med Biol 23:627–634
4. Osman S, Lundkvist C, Pike VW, Halldin C, McCarron JA, Swahn C-G, Farde L, Ginovart N, Luthra SK, Gunn RN, Bench CJ, Sargent PA, Grasby PM (1998) Nucl Med Biol 25:215–223
5. Giron MC, Portolan S, Bin A, Mazzi U, Cutler CS (2008) Q J Nucl Med Mol Imaging 52:254–266
6. Shetty HU, Zoghbi SS, Liow J-S, Ichise M, Hong J, Musachio JL, Halldin C, Seidel J, Innis RB, Pike VW (2007) Eur J Nucl Med Mol Imaging 34:667–678
7. Ma Y, Kiesewetter DO, Lang L, Gu D, Chen X (2010) Curr Drug Metab 11:483–493
8. Nakao R, Schou M, Halldin C (2012) J Chromatogr B 895–896:116–122
9. Hantraye P, Kaijima M, Prenant C, Guibert B, Sastre J, Crouzel M, Naquet R, Comar D, Maziere M (1984) Neurosci Lett 48:115–120
10. Persson A, Ehrin E, Eriksson L, Farde L, Hedström C-G, Litton J-E, Mindus P, Sedvall G (1985) J Psychiatry Res 19:609–622
11. Halldin C, Stone-Elander S, Thorell JO, Persson A, Sedvall G (1988) Appl Radiat Isot 39:993–997
12. Schou M, Steiger C, Varrone A, Guilloteau D, Halldin C (2009) Bioorg Med Chem Lett 19:4843–4845
13. Briard E, Zoghbi SS, Imaizumi M, Gourley JP, Shetty HU, Hong J, Cropley V, Fujita M, Innis RB, Pike VW (2008) J Med Chem 51:17–30
14. Nagren K, Halldin C (1998) J Label Compd Radiopharm 41:831–841
15. Briard E, Hong J, Musachio JL, Zoghbi SS, Fujita M, Imaizumi M, Cropley V, Innis RB, Pike VW (2005) J Label Compd Radiopharm 48:S71
16. Stepanov V, Krasikova R, Raus L, Loog O, Hiltunen J, Halldin C (2012) J Label Compd Radiopharm 55:206–210
17. Ma Y, Lang L, Kiesewetter D, Jagoda E, Eckelman WC (2006) Nucl Med Biol 33:1013–1019
18. Bonn B, Leandersson C, Fontaine F, Zamora I (2010) Rapid Commun Mass Spectrom 24:3127–3138
19. Levêque P, De Hoffmann E, Labar D, Gallez B (2001) J Chromatogr B 754:35–44
20. Persson A, Pauli S, Swahn C-G, Halldin C, Sedvall G (1989) Hum Psychopharmacol 4:215–220
21. Swahn C-G, Persson A, Paulis S (1989) Hum Psychopharmacol 4:297–301
22. Debruyne D, Abadie P, Barre L, Albessard F, Moulin M, Zarifian E, Baron JC (1991) Eur J Drug Metab Pharmacokinet 16:141–152
23. Prasad B, Garg A, Takwani H, Singh S (2011) Trends Anal Chem 30:360–387
24. Varrone A, Steiger C, Schou M, Takano A, Finnema SJ, Guilloteau D, Gulyás B, Halldin C (2009) Synapse 63:871–880
25. Varrone A, Tóth M, Steiger C, Takano A, Guilloteau D, Ichise M, Gulyás B, Halldin C (2011) J Nucl Med 52:132–139
26. Fujita M, Imaizumi M, Zoghbi SS, Fujimura Y, Farris AG, Suhara T, Hong J, Pike VW, Innis RB (2008) NeuroImage 40:43–52
27. Imaizumi M, Briard E, Zoghbi SS, Gourley JP, Hong J, Fujimura Y, Pike VW, Innis RB, Fujita M (2008) NeuroImage 39:1289–1298
28. Pike VW (2009) Trends Pharmacol Sci 30:431–440
29. Somers GI, Harris AJ, Bayliss MK, Houston JB (2007) Xenobiotica 37:832–854
30. De Graaf IAM, Van Meijeren CE, Pektas F, Koster HJ (2002) Drug Metab Disp 30:1129–1136